Inorganica Chimica Acta, *213* (1993) 233–246

The mercury–mercury bond in inorganic and organometallic compounds. A theoretical study

Peter Schwerdtfeger, Peter D.W. Boyd, Stephane Brienne and John S. McFeaters
The Computational Materials Science and Engineering Unit (CMSE), Department of Chemistry and School of Engineering, University of Auckland, Private Bag 92019, Auckland (New Zealand)

Michael Dolg
Institut für Theoretische Chemie, Universität Stuttgart, Pfaffenwaldring 55, D-7000 Stuttgart 80 (Germany)

M.-S. Liao and W.H. Eugen Schwarz
Theoretische Chemie, Universität Siegen, Postfach 101240, D-5900 Siegen-Weidenau (Germany)

(Received April 29, 1993)

Abstract

The effects of relativity and electron correlation in diatomic mercury HgX compounds and in linear HgX_2 and Hg_2X_2 compounds ($X=H$, F, Cl, CH_3 and CF_3) are investigated using relativistic pseudopotential and local density approximation calculations. The stability of the Hg–Hg bond in Hg_2X_2 is found to be influenced significantly by the electronegativity of the ligand X. Electronegative ligands such as fluorine ($X=F$) lead to strong mercury based radical character in the HgX monomer unit supporting an Hg–Hg bond to form a stable Hg_2X_2. This effect diminishes for less electronegative ligands such as $X=H$ or CH_3 where the unpaired electron is localized more towards the ligand X. As a consequence, Hg–Hg bonding in $Hg_2(CH_3)_2$ is very weak which may explain why organomercury compounds of the form Hg_2R_2 ($R=$any organic group) have not yet been observed. Among these organomercury compounds $Hg_2(CF_3)_2$ will be most stable. Relativistic and electron correlations effects are shown to have a significant influence on this trend. $Hg_2(CR_3)_2$ is isolobal to $Au_2(PR_3)_2$ and it is proposed that the $Hg_2(CR_3)_2$ unit may be stabilized at other metal centres.

1. Introduction

The so-called univalent state of Group 12 compounds is restricted almost entirely to the dimeric mercury unit Hg_2^{2+} forming Hg_2X_2 compounds, where X is usually an electronegative ligand [1]. In such compounds the Hg–Hg bond distances vary between 2.5 and 2.7 Å [2]. It has been speculated that this variation depends on the electronegativity of the ligand [2] (see however ref. 3). Hg–Hg binding in organomercury chemistry has been proposed [4]. However, Hg_2R_2 compounds (R being any organic ligand forming an Hg–C bond) have not yet been isolated [5] and the formation of the Hg_2^{2+} moiety appears to be strongly dependent on the chosen ligand X. The reason for this behavior is not yet understood, and even a qualitative explanation of this unique feature has yet to be put forward. Moreover, preliminary theoretical studies on gas phase Hg_2^{2+} suggest that this species is only metastable in the free state, but becomes stabilized in a polar surrounding, where it is relativistically destabilized [3, 6–9] somewhat in contrast to the isoelectronic Au_2 molecule, which is strongly stabilized by relativity [10–12].

It is well known that relativistic effects play a very important role in gold compounds [10–14]. The first and second ionization potentials for the Group 12 elements are shown in Fig. 1. Both relativistic and lanthanide contraction effects are responsible for the anomaly in the observed ionization potentials, as is the case for the Group 11 elements [10]. The relatively large ionization potential of mercury compared to cadmium or zinc is often seen as the reason for the chemical inertness of mercury [1]. Since bonding in mercury compounds is expected to be mainly due to covalent overlap interactions of the Hg(6s) orbitals, which are strongly contracted and stabilized by relativity, we expect relativistic effects to be important in the chemistry of mercury. For example, anomalies in the M–X stretching force constants (X = halogen) of the Group 12 halides MX_2 (M = Zn, Cd, Hg) are assumed to be due to relativistic effects [17]. The anomalous high superconducting transition temperature of mercury ($T_c=4.15$

0020-1693/93/$6.00

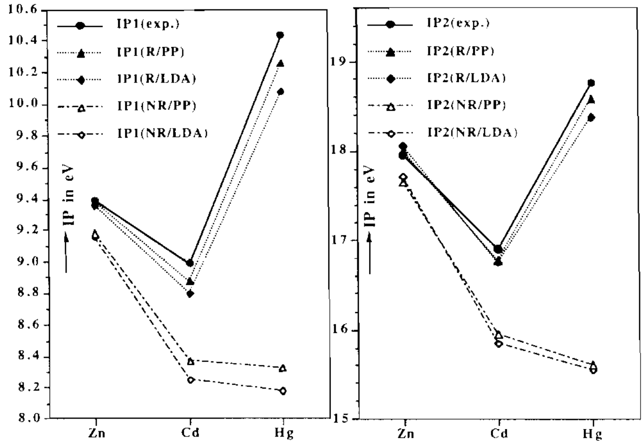

Fig. 1. First (left side) and second (right side) ionization potentials of the Group 12 elements (in eV). Experimental values from ref. 15. The relativistic (R) and non-relativistic (NR) values are from pseudopotential QCI (using basis set L for Hg and similar basis sets for Zn and Cd, see ref. 16) and from LDA calculations. First ionization potentials IP1 (in eV): Zn 9.391 (exp.), 9.383 (R/PP), 9.360 (R/LDA), 9.185 (NR/PP), 9.163 (NR/LDA); Cd 8.991 (exp.), 8.872 (R/PP), 8.793 (R/LDA), 8.369 (NR/PP), 8.250 (NR/LDA); Hg 10.430 (exp.), 10.249 (R/PP), 10.069 (R/LDA), 8.325 (NR/PP), 8.174 (NR/LDA). Second ionization potentials IP2 (in eV): Zn 17.960 (exp.), 17.990 (R/PP), 18.062 (R/LDA), 17.652 (NR/PP), 17.713 (NR/LDA); Cd 16.904 (exp.), 16.779 (R/PP), 16.743 (R/LDA), 15.942 (NR/PP), 15.843 (NR/LDA); Hg 18.751 (exp.), 18.581 (R/PP), 18.376 (R/LDA), 15.601 (NR/PP), 15.542 (NR/LDA).

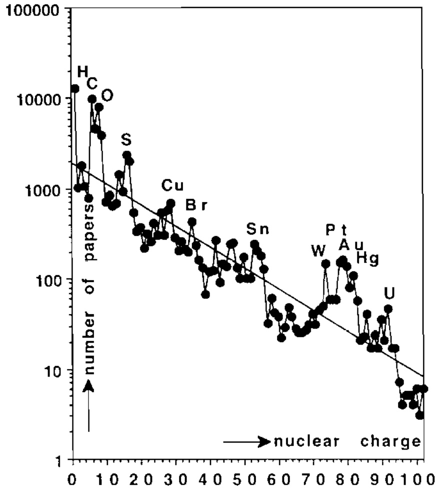

Fig. 2. Number of published papers in the period between 1978 and 1991 for atoms and molecules containing specified elements. Only *ab initio* and local density results are considered. The numbers have been obtained from the QCLDB library (ref. 18).

K) compared to zinc ($T_c = 0.85$ K) or cadmium ($T_c = 0.52$ K) may be due to relativistic effects [12]. The same may hold for the anomalously low melting point of mercury [10].

First-principle all-electron calculations including relativistic and electron correlation effects for larger molecules containing heavy elements are very demanding computationally and are not yet feasible even with present day parallel or vector computers. Since the computation time is critically dependent on the number of electrons involved when solving the Schrödinger equation (or its relativistic analogue, the Dirac equation), it is understandable that most theoretical investigations are concerned with small molecules containing only the lighter elements in the Periodic Table, as exhibited in Fig. 2. For large molecules containing heavy elements, the local density functional (LDA) [19] and the pseudopotential (PP) [20] approximations appear to be the only available quantum chemical methods that yield reliable enough results to be of chemical relevance in the present context. Efficient and versatile software packages are now available for both approaches and improvements in algorithms and computer power open the way for the study of larger sized molecules including clusters of heavy elements.

Das and Wahl undertook the first studies of relativistic effects in mercury compounds using non-relativistic and relativistic spin–orbit averaged [$6s^2$] pseudopotentials [21]. In more recent work, relativistic effects on small mercury compounds have been investigated in detail [22–27]. In a recent paper it has been demonstrated that multi-electron adjusted [$5s^25p^65d^{10}6s^2$] pseudopotentials for mercury lead to accurate results for the ground and excited states of HgH [28]. The local density approximation has been applied to a number of mercury containing molecules [3, 7, 29, 30]. Dewar *et al.* reported AM1 and MNDO results for a large series of mercury compounds [31].

The pseudopotentials, the local density functionals and the basis sets used in the present work are described in detail in the next section. The atomic and molecular calculations are presented and discussed in Section 3. Our conclusion is given in Section 4.

2. Method

The Pseudopotential approximation

The pseudovalence Hamiltonian is defined as follows

$$\bar{H} = -\frac{1}{2}\sum_i \Delta_i + \sum_{\lambda<\mu}\frac{Q_\lambda Q_\mu}{r_{\lambda\mu}} + \sum_{i<j}\frac{1}{r_{ij}} - \sum_{\lambda,i}\frac{Q_\lambda}{r_{\lambda i}} + V_{PP} \qquad (1)$$

where V_{PP} is the pseudopotential for the molecule, Q_λ is the charge of the core λ ($Q_{Hg} = 20$ for a [$Kr4d^{10}4f^{14}$]-core definition), i,j and λ,μ are the valence electron and atomic core indices, respectively. V_{PP} is given by the following sum

$$V_{PP}=\sum_{\lambda}\left(V^{\lambda}_{PP}+V^{\lambda}_{CPP}+\sum_{\mu<\lambda}V^{\lambda\mu}_{CCR}\right) \qquad (2)$$

where V_{PP} is the atomic core pseudopotential, V^{λ}_{CPP} the atomic core polarization potential of the atom λ and $V^{\lambda\mu}_{CCR}$ is the atomic core–core repulsion correction for atoms λ and μ ($V_{PP}=0$ and $Q_{\mu}=Z_{\mu}$ if no frozen core is introduced for atom μ and all electrons are treated explicitly). V_{PP} is chosen to have the following functional form [27, 32]

$$V^{\lambda}_{PP}=\sum_{i}\sum_{l<l_{max}}(A_{l\lambda}\exp(-a_{l\lambda}r^{2}_{\lambda i}) + B_{l\lambda}\exp(-b_{l\lambda}r^{2}_{\lambda i}))\sum_{m_l}|\lambda l m_l\rangle\langle\lambda l m_l| \qquad (3)$$

For the core of Hg defined as [Kr4d^{10}4f^{14}], V^{Hg}_{CPP} and V^{HgHg}_{CCR} are small enough to be neglected. The pseudopotential parameters for Hg were published in ref. 27.

Several earlier papers on mercury compounds accounted only for the 6s^2 valence electrons within a pseudopotential approximation for the mercury atom assuming the 5d shell to be frozen [21–23,33]. This might at first seem to be justified since, for example, Xα calculations on $Hg(CH_3)_2$ by DeKock *et al.* have shown that 5d excitations calculated for the $Hg(CH_3)_2$ photoelectron spectra are atomic like [29]. On the other hand, it has been demonstrated in a recent paper on $M(CH_3)_2$ compounds ($M=Au^-$, Hg, Tl^+ and Pb^{2+}) by one of the present authors that excitations of the 5d core in a configuration expansion contribute significantly to the correlation corrections of the mercury–ligand stretching force constant [34]. Basch *et al.* noted that for accurate HF calculations on mercury compounds an [Xe4f^{14}]-core ($Q_{Hg}=12$) definition including the 5d electrons in the valence space is more appropriate than a [Pt]-core ($Q_{Hg}=2$) [23]. Keeping the Hg(5d) electrons frozen leads to errors mainly because of the incorrect description of core–core repulsion and of neglect of core polarization (core–valence correlation) [35–37]. However, for larger molecules or cluster compounds the use of a small core definition for mercury may become computationally too demanding. It is therefore of interest to examine if a two-valence electron pseudopotential approximation for mercury, if corrected for core–core repulsion and core polarization, can lead to reasonably accurate molecular properties. A [Pt]-core definition including the necessary corrections is therefore highly desirable. Such corrections have been used with some success for several other metal containing compounds [32, 36–39].

At small internuclear mercury–ligand distances the ligand core penetrates the Hg(5d) shell. This gives rise to deviations from a point-charge Coulomb interaction between the ligand and the [Pt]-core of mercury. Such effects have been calculated earlier by Schwarz [36] and by Stoll *et al.* for copper and silver compounds [37]. The calculated core–core repulsion corrections are depicted in Fig. 3 for the metal–metal interactions of Au_2, Hg_2 and Tl_2. For atoms with not too large dipole polarizabilities α_D of the core, as is the case for the [Pt]-core for thallium, lead or heavier atoms, core-valence correlation may be simulated by a core polarization potential [35]. The molecular properties obtained using such an approach are in excellent agreement with experimental results [28, 32, 39]. For very polarizable cores such as the [Pt]-'core' of gold, however, such an approximation turned out to be too crude concerning several molecular properties [33]. The dipole polarizability of Hg^{2+} ($\alpha_D=1.25$ Å^3) [40] is only slightly smaller than that of Au^+ ($\alpha_D=1.72$ Å^3) [41]. Figure 3 shows that at typical Hg–Hg distances (2.5 Å) core–core repulsion effects (V^{HgHg}_{CCR}) can be as large as 70 kJ/mol at the relativistic level, which is a significant contribution to the Hg–Hg dissociation energy of about 200 kJ/mol. Certainly, Hg_2, which is a van der Waals system with a dissociation energy of around 4 kJ/mol [42] (see ref. 43 for more details), cannot be described satisfactorily using a frozen [Pt]-core. Core–valence correlation effects for Hg_2H_2 at the MP2 level are large, e.g. the Hg–Hg bond distance decreases by 0.1 Å due to electron correlation of the mercury 5d shells. Therefore, we have chosen a [Kr4d^{10}4f^{14}]-core pseudopotential for mercury, adjusted by a multi-electron fit-procedure to non-relativistic and relativistic Hartree-Fock levels [27].

We have performed pseudopotential Hartree-Fock (HF) and Møller-Plesset second-order (MP2) calcu-

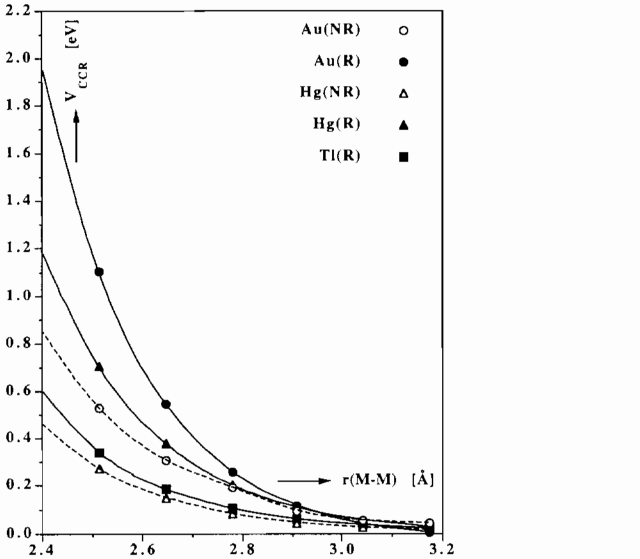

Fig. 3. Core–core repulsion corrections (CCR) for several diatomic molecules. The method of calculation is described in ref. 33.

lations for the compounds HgX, HgX_2 and Hg_2X_2 (X = H, F, Cl, CH_3 and CF_3). For Hg a contracted (9s,7p,6d,1f) basis set with contraction scheme (21111111/22111/3111/1) and exponents given in ref. 27 was used, the exponent of an additional diffuse s-function being 0.005. For H we used a (10s,2p)/[7s,2p], and for F a 6-311+G* basis, for C a 6-311G* basis [44]. We denote this standard basis set as S. For the H atom of the methyl group and for the F atom of the CF_3 group we had to reduce the basis sets to a 411G and a STO-3G set [44, 45], respectively, because the geometry optimizations for $Hg_2(CH_3)_2$ and $Hg_2(CF_3)_2$ became rather time consuming. Since the STO-3G basis set of F is unbalanced compared to the relatively large basis sets of C and Hg, leading to unreasonable dipole moments and atomic charges, the Mulliken population analysis as well as the dipole moments have been recalculated with the larger F basis set at the optimized geometries of $HgCF_3$, $Hg(CF_3)_2$ and $Hg_2(CF_3)_2$. For $Hg_2(CF_3)_2$ this leads to 406 primitive gaussians contracted to 268 basis functions.

For the more sophisticated pseudopotential calculations of the mercury compounds HgH^+, HgH and HgH_2 at the theoretical levels of HF, MP*n* ($n = 2$, 3, 4; MP4 includes all singles, doubles, triples and quadruples contributions), CISD (configuration interaction singles–doubles) and QCI [quadratic CI [QCISD(T)] [46]), we used a larger (9s, 8p, 7d, 2f)/[8s, 6p, 5d, 2f] basis with contraction scheme (21111111/221111/31111/11) and exponents as described in ref. 27 (denoted as basis set L). The L basis was also used for MP2 calculations of Hg_2, Hg_2^+ and Hg_2^{2+}. We found that basis S leads only to negligible changes compared to basis L for Hg_2H_2 at the HF level. The GAUSSIAN86/88/90/92 program packages have been used for all calculations [44, 47].

The local density approximation

Density functional calculations using the frozen atomic core approximation and the LC-STO expansion technique have been performed with the Amsterdam AMOL program package [48]. The correlation energy was accounted for by the local functional of Vosko *et al.* [49]. The exchange energy was corrected by Becke's recipe [50] in several preliminary calculations. However, we found significantly large bond lengths and low bond energies (as in some other heavy atom compounds from Group 11) [3]. Concerning the correlation correction, it seems to improve the results more or less. Since these improvements are not large in most cases, and since it has been argued to apply correlation and exchange corrections only simultaneously (e.g. see ref. 52), we have decided to present only the simple $X\alpha$-type results ($\alpha = 0.7$) in the Tables [51]. Relativity, as presented in the Tables, has been accounted for at the Dirac-Fock level in the atomic cores, and by first-order perturbation theory in the valence shells. So at this level of theory the influence of relativistic orbital relaxation in the valence shells on the molecular properties is not fully taken into account.

The optimized Slater type basis sets of Baerends and co-workers have been applied [53]. For mercury we use a [Xe]-core with a single-ζ basis for the core wiggles of the valence orbitals and a triple-ζ basis for the 5d and 6s shells. Two p-polarization functions were added ($\zeta = 2.6$ and 1.35). An additional f-polarization function changes the Hg–Hg bond lengths by about 2 pm and its bond energy by about 0.1 eV, while the Hg–X bonds are influenced even less. Therefore it has been omitted from the main series of calculations. For carbon and fluorine (chlorine) we used a [He]-core ([Ne]-core), a single-ζ set for the core wiggles of the valence shells, a double-ζ set for the valence s and p shells, and the following d-polarization functions: 3d($\zeta = 1.8$) for C, 3d($\zeta = 1.5$) for F and 3d($\zeta = 1.8$) for Cl. A somewhat larger exponent for the F(3d) function may seem more appropriate; however, the results are changed only insignificantly. For hydrogen two 1s and a 2p($\zeta = 1.0$) function were included.

3. Results and discussion

Performance of the methods

A measure of the performance of the different approximations used can be obtained from the values listed in Table 1 for the mercury hydrides HgH^+, HgH and HgH_2. Both, the correlated corrected pseudopotential methods, especially at the highest level of electron correlation (QCI), and the local density approximation perform reasonably well if compared with experimental data (bond lengths ± few pm, bond energies ± few tens kJ/mol, force constants ± few 0.1 mdyn/Å). Except for the dissociation energy of the weakly bound HgH molecule, the MP2 method gives reasonable results. It is well known that the MP procedure converges slowly for transition element compounds, and it was shown recently that large basis sets including more f- as well as g-functions within a multi-reference CI procedure is necessary to obtain a reasonably accurate value of the HgH dissociation energy [28]. Note that the LDA approximation yields reasonable value for the dissociation energy at low computational cost. In particular no high angular momentum basis functions are needed to account for the important correlation effects.

Concerning the molecular radicals HgX in Table 2, the results show similar trends. However, the pseudopotential HF and MP2 results of the Hg–CH_3 bond length seem too large, while the relativistic perturbative LDA calculation may slightly underestimate the value:

TABLE 1. Molecular properties of HgH^+, HgH and HgH_2 at the relativistic level of theory using basis set L[a]

Molecule		HF	MP2	MP3	MP4	CISD	CISDSC	QCI	LDA	Exp.
HgH^+	r_e	1:622	1.566	1.592	1.590	1.587	1.591	1.596	1.62	1.594
	D_e	121.0	236.0	225.0	252.7	208.2	236.7	250.2	280	(301)
	k_e	2.47	2.70	2.46	2.41	2.60	2.47	2.34	2.27	2.43
HgH	r_e	1.773	1.739	1.745	1.754	1.742	1.744	1.768	1.81	1.766
	D_e	16.6	−0.8	23.7	22.3	22.6	26.5	29.2	48	43.3
	k_e	1.02	0.92	1.09	0.97	1.09	0.97	0.91	0.92	0.86
	IP	7.42	8.00	7.86	7.95	7.79	7.89	7.96	7.44	(7.0)
HgH_2	r_e	1.660	1.617	1.636	1.634	1.632	1.636	1.641	1.70	
	D_e	252.2	307.9	337.7	340.3	320.0	339.6	342.7	367	
	k_e	2.52	2.90	2.65	2.64	2.72	2.64	2.52	2.20	

[a] Equilibrium distances r_e in Å, binding energies D_e in kJ/mol (zero-point vibrational contributions are not included), symmetric stretching force constants k_e in mdyn/Å and adiabatic ionization potentials IP for HgH in eV. Experimental values from ref. 54.

TABLE 2. Molecular properties of HgH, HgF, HgCl, $HgCH_3$ and $HgCF_3$[a]

Molecule		r_e		D_e		k_e		μ_e	
		NR	R	NR	R	NR	R	NR	R
HgH	HF	1.886	1.774	73.2	16.8	1.20	1.00	1.22	0.52
	MP2	1.826	1.727	53.1	6.2	1.29	1.02	0.97	0.19
	LDA	1.94	1.81	87	48	0.80	0.92	0.62	0.12
	exp.		1.766		43.3		1.04		
HgF	HF	2.109	2.045	169.7	28.5	2.38	2.36	4.64	4.22
	MP2	2.110	2.045	236.0	91.8	2.27	2.02	4.56	3.58
	LDA	2.12	2.10	300	203	2.20	1.97	3.49	3.00
	exp.				(175)		2.46		
HgCl	HF	2.504	2.422	192.9	69.7	1.86	1.82	4.85	4.13
	MP2	2.450	2.375	178.1	57.9	1.63	1.87	4.32	3.03
	LDA	2.50	2.46	208	129	1.36	1.22	3.65	2.74
	exp.				102		1.50		
$HgCH_3$	HF	2.381	4.940	4.8	0.7	1.15	0.002	0.34	−0.13
	MP2	2.308	3.542	31.8	4.9	1.32	0.04	0.003	−0.27
	LDA	2.36	2.27	60	19	0.94	0.97	0.18	−0.48
	exp.				29				
$HgCF_3$	HF	2.391	2.374	99.0	91.6	0.83	0.47	2.85	1.17
	MP2	2.290	2.213	147.2	151.3	1.21	0.94	1.74	−0.13
	LDA	2.51	2.44	50	10	0.54	0.44	1.26	0.61

[a] Equilibrium distances r_e in Å, binding energies D_e in kJ/mol (zero-point vibrational contributions are not included), force constants k_e in mdyn/Å and dipole moments μ_e in D (positive sign in μ_e corresponds to $Hg^{\delta+}L^{\delta-}$). The (...5s5p) electrons of Hg, the (1s) cores of F and C and the (1s2s2p) core of Cl have been kept frozen in the MP2 calculations of $HgCH_3$ and $HgCF_3$ and in all LDA calculations. Experimental values from refs. 5 and 54. Additional geometric parameters (in Å and °): $HgCH_3$: NRHF $r_e(CH)=1.085$, $\alpha_e(HgCH)=109.0$; RHF $r_e(CH)=1.073$, $\alpha_e(HgCH)=90.6$; NRMP2 $r_e(CH)=1.093$, $\alpha_e(HgCH)=108.1$; RMP2 $r_e(CH)=1.081$, $\alpha_e(HgCH)=91.1$. $HgCF_3$: NRHF $r_e(CF)=1.285$, $\alpha_e(HgCF)=109.8$; RHF $r_e(CF)=1.278$, $\alpha_e(HgCF)=108.3$; NRMP2 $r_e(CF)=1.290$, $\alpha_e(HgCF)=108.6$; RMP2 $r_e(CF)=1.286$, $\alpha_e(HgCF)=107.7$. CH_3: HF $r_e(CH)=1.074$, $\alpha_e(HCH)=120.0$; MP2 $r_e(CH)=1.080$, $\alpha_e(HCH)=120.0$. CF_3: HF $r_e(CF)=1.271$, $\alpha_e(FCF)=111.6$; MP2 $r_e(CF)=1.278$, $\alpha_e(FCF)=111.8$.

relaxation of the valence shell due to relativity (Hg(6s) orbital contraction) extends(!) the bond length by 0.1 Å. The HF and MP2 bond energies of Hg–CF_3 are unexpectedly large in comparison to the more systematic LDA value. The AM1 and MNDO calculations by Dewar and co-workers [31] give very short bond distances for HgF (1.87 Å) and HgCl (2.23 Å) as compared to both the present pseudopotential and LDA results (difference of *c.* 0.2 Å). There are no experimental bond distances available for these two species. One might argue that larger basis sets and more sophisticated electron correlation procedures are necessary to obtain shorter bond distances. A comparison between the two different basis sets used for the molecules HgH and HgH_2 (Tables 1, 2 and 3), however, shows that the larger basis gives similar results as the standard basis at both the HF and MP2 levels of theory. The present Hartree-Fock CF bond distance of 1.298 Å and FCF angle of 107.4° of the trifluoromethyl compounds are in reasonable agreement with Oberhammer's gas phase electron difraction measurements of 1.345 Å and 106.8°, respectively [55].

From the results on HgX_2 compounds in Table 3 we again see that the pseudopotential HF and MP2 bond energies are rather low in comparison to the LDA values except for the trifluoromethyl compound, where the pseudopotential HF value is very large. Also the corresponding force constant is unexpectedly large, while the LDA reproduces the trend of $k(Hg(CH_3)_2) > k(Hg(CF_3)_2)$ [56]. The LDA bond lengths in general tend to be large by several pm. The experimental bond length of gas phase $HgCl_2$ [54] (Table 3) is in very good agreement with our MP2 result.

The Hg_2 compounds are displayed in Table 4. There is only crystal structure data available for Hg_2F_2 and Hg_2Cl_2. Comparative LDA calculations on the molecular and solid halides have indicated an expansion of the Hg–X bonds in the crystal due to interactions with adjacent halogen atoms [3] by about 0.1 Å, while the Hg–Hg bonds are changed insignificantly in the condensed phase. Furthermore the presented LDA results probably overestimate the Hg–Hg bond distances by *c.* 2 pm because of the neglect of f-functions. It is hard to say whether the longer HF and LDA results or the shorter MP2 values are the better ones. Note that different experimentalists [2, 58] favour different bond lengths. Perhaps larger basis sets and a more sophisticated electron correlation procedure than MP2 are necessary to obtain shorter mercury–ligand bond distances. The GVB results of Kleier and Wadt [26] on Hg_2Cl_2 support the LDA distances and the experimental values of ref. 58, while their dissociation energies are surely underestimated. In general the LDA Hg–Hg bond energies lie between the smaller HF and the larger MP2 pseudopotential values. Again the pseudopotential approach predicts an exceptional stability for the trifluoromethyl compound.

Relativistic effects

Relativistic effects in mercury hydrides have been discussed extensively in ref. 28. The mercury bond distances decrease in general due to relativistic effects, as may be naively expected from the relativistic Hg(6s) contraction (see, however, the discussion in refs. 10 and 11). The relativistic bond contractions $\Delta_R r_e = r_e^{NR} - r_e^{R}$ do not vary much within a series of HgX_2 and Hg_2X_2 compounds. Concerning the Hg–X bond lengths, $\Delta_R r_e$ is about 9 pm at the LDA level and 12 pm (14 pm) at the pseudopotential MP2 (HF) levels. The Hg–Hg bonds contract twice as much, i.e. by about 0.2 (LDA), 0.25 (MP2) and 0.3 (HF) Å. Relativistic changes in r_e are smaller in the Hg–X radical compounds. The $Hg–CH_3$ bond may even be relativistically expanded, as discussed above. Summa-

TABLE 3. Molecular properties of HgH_2, HgF_2, $HgCl_2$, $Hg(CH_3)_2$ and $Hg(CF_3)_2$[a]

Molecule		r_e		D_e		k_e		ΔU_0	
		NR	R	NR	R	NR	R	NR	R
HgH_2	HF	1.815	1.663	278.6	252.3	2.19	3.10	5.6	−59.7
	MP2	1.747	1.615	335.5	318.8	1.92	2.91	4.2	−52.4
	LDA	1.81	1.70	378	367	1.62	2.20	−6	−42
HgF_2	HF	2.056	1.931	409.5	229.8	3.08	3.95	71.5	24.6
	MP2	2.042	1.918	637.3	461.1	2.69	3.71	77.6	35.3
	LDA	2.04	1.97	751	627	2.95	3.35	61	42
$HgCl_2$	HF	2.428	2.298	464.5	309.5	2.49	3.23	61.0	12.4
	MP2	2.369	2.245	533.9	394.0	1.93	2.93	67.1	19.7
	LDA	2.40	2.31	567	467	1.95	2.29	55	31
	exp.		2.252						
$Hg(CH_3)_2$	HF	2.277	2.127	131.8	108.0	1.70	2.38	5.1	−62.0
	MP2	2.211	2.080	279.0	264.0	1.88	2.63	1.9	−54.5
	LDA	2.25	2.14	303	286	1.61	2.10	−3	−98
	exp.		2.083		243		2.38		
$Hg(CF_3)_2$	HF	2.202	2.066	334.6	382.9	2.32	3.13	50.5	−26.5
	LDA	2.34	2.21	251	224	1.22	1.62	−8	−78
	exp.		2.101				2.18		

[a] Equilibrium distances r_e in Å, binding energies D_e in kJ/mol (zero-point vibrational contributions are not included), symmetric stretching force constants k_e in mdyn/Å and reaction energies $\Delta U_0(Hg_2L_2 \rightarrow HgL_2 + Hg)$ in kJ/mol. The (...5s5p) electrons of Hg, the (1s) cores of C and F and the (1s2s2p) core of Cl have been kept frozen in the MP2 calculations of $Hg(CF_3)_2$ and in all LDA calculations. Experimental values from refs. 5, 54–56. Additional geometric parameters (in Å and °): $Hg(CH_3)_2$: RHF $r_e(CH) = 1.086$, $\alpha_e(HgCH) = 111.0$; NRHF $r_e(CH) = 1.087$, $\alpha_e(HgCH) = 111.2$; RMP2 $r_e(CH) = 1.095$, $\alpha_e(HgCH) = 111.4$; NRMP2 $r_e(CH) = 1.095$, $\alpha_e(HgCH) = 110.6$. $Hg(CF_3)_2$: RHF $r_e(CF) = 1.298$, $\alpha_e(HgCF) = 111.5$; NRHF $r_e(CF) = 1.300$, $\alpha_e(HgCF) = 112.0$.

TABLE 4. Molecular properties of the mercury dimers Hg_2H_2, Hg_2F_2, Hg_2Cl_2, $Hg_2(CH_3)_2$ and $Hg_2(CF_3)_2$[a]

Molecule		r_e^{Hg-Hg}	r_e^{Hg-X}	D_e	k_e^{Hg-Hg}	k_e^{Hg-X}
Hg_2H_2	HF	2.705(2.995)	1.696(1.853)	159.0(137.7)	1.30(0.74)	2.05(1.54)
	MP2	2.603(2.822)	1.643(1.784)	254.3(233.5)	1.75(1.02)	2.05(1.69)
	LDA	2.73(2.92)	1.74(1.86)	208(179)	1.13(0.80)	1.95(1.39)
Hg_2F_2	HF	2.591(2.914)	1.994(2.085)	197.3(141.5)	1.67(0.91)	3.05(2.46)
	MP2	2.488(2.740)	1.977(2.074)	312.8(243.0)	2.46(1.30)	3.65(2.46)
	LDA	2.60(2.81)	2.04(2.09)	265(211)	1.57(1.06)	3.48(2.58)
	exp.[b]	(2.507)	(2.14)			
	GVB[c]	2.56	1.97	189		
Hg_2Cl_2	HF	2.627(2.938)	2.354(2.469)	182.4(139.7)	1.56(0.82)	2.07(1.68)
	MP2	2.518(2.761)	2.295(2.410)	297.9(244.8)	2.13(1.24)	2.44(2.50)
	LDA	2.63(2.84)	2.37(2.45)	239(206)	1.54(0.80)	1.99(1.95)
	exp.[b]	(2.526)	2.43			
	exp.[d]	(2.595)	2.362			
	GVB[c]	2.60	2.33	172		
$Hg_2(CH_3)_2$	HF	2.703(2.995)	2.167(2.331)	44.6(127.2)	1.26(0.69)	2.05(1.63)
	MP2	2.614(2.839)	2.113(2.247)	200.5(217.4)	1.56(1.12)	2.25(1.56)
	LDA	2.72(2.92)	2.22(2.30)	150(180)	1.03(0.73)	1.65(1.39)
$Hg_2(CF_3)_2$	HF	2.657(2.898)	2.104(2.240)	173.2(187.2)	1.56(0.95)	2.77(2.33)
	LDA	2.73(2.93)	2.31(2.39)	126(158)	1.13(0.79)	1.10(1.03)

[a] Equilibrium distances r_e in Å, dissociation energies $D_e(Hg_2X_2 \rightarrow 2HgX)$ in kJ/mol and symmetric stretching force constants k_e (per bond) in mdyn/Å. Non-relativistic values are set in brackets. The (...5s5p) electrons of Hg, the (1s) cores of C and F and the (1s2s2p) core of Cl have been kept frozen in the MP2 calculations of $Hg_2(CF_3)_2$ and in all LDA calculations. Additional geometric parameters (in Å and °): $Hg_2(CH_3)_2$: RMP2 $r_e(CH) = 1.095$, $\alpha_e(HgCH) = 110.0$; NRMP2 $r_e(CH) = 1.095$, $\alpha_e(HgCH) = 110.6$; RHF $r_e(CH) = 1.086$, $\alpha_e(HgCH) = 110.8$; NRHF $r_e(CH) = 1.089$, $\alpha_e(HgCH) = 111.3$. $Hg_2(CF_3)_2$: RHF $r_e(CF) = 1.299$, $\alpha_e(HgCF) = 111.4$; NRHF $r_e(CF) = 1.304$, $\alpha_e(HgCF) = 112.0$. [b] Experimental values from single crystal data by Dorm (ref. 2). [c] Two configuration SCF (generalized valence bond) calculations by Kleier and Wadt (ref. 26). [d] More recent crystal powder neutron diffraction experiment (ref. 58).

rizing, the mercury bond contracts relativistically by about 5% in Hg(II) compounds, and by 10% in the case of the Hg–Hg bond. This is still not big enough to cause anomalies within the Group 12 series of compounds, in contrast to Group 11 containing molecules [3, 12].

The Hg–X and especially the Hg–Hg stretching force constants in the HgX_2 and Hg_2X_2 compounds undergo so large a relativistic increase (Tables 3 and 4) that an anomaly in the trend of the Group 12 stretching force constants occurs, as was already mentioned earlier in ref. 17. In contrast, the HgX compounds show small positive or negative relativistic changes in k_e, as for the $\Delta_R r_e$ values discussed above, and a normal trend is observed for this property along the Group 12 series of compounds [17].

Although relativity reduces the length and increases the force constant of Hg–X bonds, at least in the HgX_2 and Hg_2X_2 compounds, the bond dissociation energies are relativistically reduced (see Tables 2 and 3). The magnitude of this effect increases dramatically from the less electronegative ligands CH_3 and H to the more electronegative ones, Cl and F. The opposite trend occurs for the Hg–Hg bond, which is relativistically destabilized for CH_3 and CF_3, but relativistically stabilized for H and especially for Cl and F.

Stability of the mercury–mercury bond

Figure 4 shows MP2 potential curves for Hg_2, Hg_2^+ and Hg_2^{2+}. Only Hg_2^+ shows a significantly large dissociation energy, Hg_2 is a van der Waals molecule and Hg_2^{2+} is metastable in the gas phase. Neisler and Pitzer showed that the stability of the Hg_2^{2+} unit is caused by solvent stabilization, i.e. hydration stabilizes the Hg_2^{2+} ion by *c.* 260 kcal/mol [8]. This energy is much larger than the negative dissociation energy of free Hg_2^{2+}. Nevertheless, the sequence in stability along the series Hg_2, Hg_2^+ and Hg_2^{2+} suggests that the electronegativity or polarity of the ligand X in Hg_2X_2

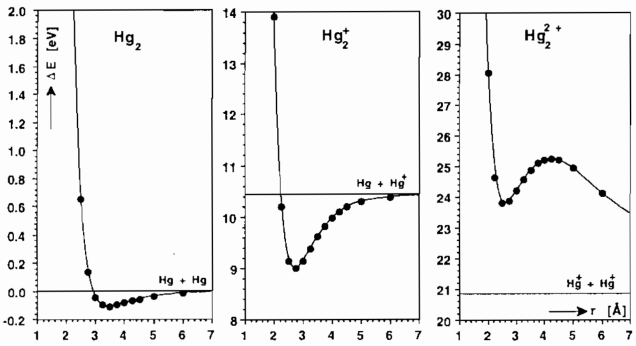

Fig. 4. Relativistic MP2 potential curves for Hg_2, Hg_2^+ and Hg_2^{2+} (in eV). The dissociation limit is shown by a straight line for each potential curve.

compounds will play a major role for the strength of the Hg–Hg bond.

The dissociation energy of Hg_2X_2 into two HgX units (Table 5) shows the following sequence in stability for the Hg–Hg bond: $Hg_2F_2 > Hg_2Cl_2 > Hg_2H_2 > Hg_2(CH_3)_2$. This is (more or less) expected from the sequence in the ligand electronegativity [59] $F > CF_3 > Cl > CH_3 \sim H$. Concerning $Hg_2(CF_3)_2$ the pseudopotential HF value indicates that the electron-attractive ligand CF_3 stabilizes the Hg–Hg bond significantly, $Hg_2(CF_3)_2$ being more stable than both Hg_2H_2 and $Hg_2(CH_3)_2$ by over 30 kJ/mol. On the other hand the LDA predicts $Hg_2(CH_3)_2$ to be less stable than Hg_2H_2 by more than 30 kJ/mol, and $Hg_2(CF_3)_2$ to be of intermediate instability.

The decomposition energy ΔU_0 for the disproportionation reaction

$$Hg_2X_2 \rightarrow HgX_2 + Hg \tag{4}$$

is another measure of the stability of Hg_2X_2 species. The reaction energies ΔU_0 (see (5)) are listed in Table 5 and are depicted in Fig. 5. Reaction (4) leading to gaseous Hg is endothermic by about 20 to 40 kJ/mol for the electropositive ligands (F, Cl), and exothermic for the 'electroneutral' ones (H, R). If reaction (4) yields liquid Hg, however, the energies are *c*. 60 kJ/mol more exothermic [40], thereby shifting all ΔU_0 energies to negative values. The trend in ΔU_0 calculated is similar to the trend in the Hg_2X_2 dissociation energies discussed above, i.e. $Hg_2F_2 > Hg_2Cl_2 > Hg_2(CF_3)_2 > Hg_2H_2 \sim Hg_2(CH_3)_2$.

$$\begin{tikzcd}
Hg_2X_2 \arrow[r, "D_e^1"] \arrow[d, "\Delta U_0"] & 2HgX \arrow[d, "2D_e^2"] \\
Hg + HgX_2 \arrow[r, "D_e^3"] & 2Hg + 2X
\end{tikzcd} \tag{5}$$

The theoretical trends reflect what is known experimentally, namely that Hg_2F_2 has been definitely isolated and that organometallic compounds of the general form Hg_2R_2 (R any organic ligand) are unknown. Relativistic effects stabilize the Hg–Hg bond significantly for electronegative ligands. Hence relativistic effects are partly responsible for the unique occurrence of the Hg_2^{2+} unit within the Group 12 series of compounds if bound to electron attracting groups.

Scheme (5) shows that $\Delta U_0 = D_e^1 + 2D_e^2 - D_e^3$. The relativistic contribution to ΔU_0, $\Delta_R\Delta U_0 = \Delta U_0^{NR} - \Delta U_0^R$, can therefore be traced back to the individual dissociation energies D_e^1, D_e^2 and D_e^3. The relativistic changes in these contributions are listed in Table 5 at the HF, MP2 and LDA level of theory. The ΔU_0 values for reaction (4) *all* show a relativistic decrease which is, however, much larger for the electroneutral ligands. Hence, relativistic effects support the disproportionation reaction (4) of all Hg_2X_2 compounds, but more strongly in the case of non-electron attracting ligands.

Mulliken population analyses, orbital energies and electron densities

The Mulliken population analyses of the pseudopotential MP2 calculations are shown in Tables 6 and 7. The atomic charges on Hg vary with the ligand according to the order $F > Cl > H, CH_3 > CF_3$. The same trend is found in the HF as well as in the LDA calculations. It is remarkable that this order differs from the order of ligand electronegativities [59] mentioned above, while Dewar's atomic charges from his AM1 and MNDO calculations [31] correlate well with the ligands' electronegativities. It is well known that Mulliken's population analysis is rather dependent on the method and basis chosen. Nevertheless, we may summarize the following important features.

TABLE 5. Relativistic dissociation energies as defined in (5) (and relativistic contributions $\Delta_R D_e = D_e^{NR} - D_e^R$ to them in parentheses) at the HF, MP2 and LDA levels of theory (in kJ/mol)

Molecule		$D_e^1(\Delta_R D_e^1)$	$2D_e^2(2\Delta_R D_e^2)$	$D_e^3(\Delta_R D_e^3)$	$\Delta U_0(\Delta_R \Delta U_0)$
Hg_2F_2	HF	197(−56)	57(282)	230(180)	24(47)
	MP2	313(−70)	184(288)	461(176)	36(42)
	LDA	265(−54)	406(194)	627(124)	43(17)
Hg_2Cl_2	HF	182(−43)	140(246)	310(155)	12(49)
	MP2	298(−53)	116(240)	394(140)	20(47)
	LDA	239(−34)	258(158)	467(100)	30(24)
Hg_2H_2	HF	159(−21)	33(113)	252(26)	−60(65)
	MP2	254(−21)	12(94)	319(17)	−53(56)
	LDA	208(−29)	96(78)	367(11)	−63(38)
$Hg_2(CH_3)_2$	HF	45(83)	1(8)	108(24)	−62(67)
	MP2	200(17)	10(54)	264(15)	−54(57)
	LDA	150(30)	38(82)	286(17)	−98(96)
$Hg_2(CF_3)_2$	HF	173(14)	183(15)	383(−48)	−27(77)
	LDA	126(32)	20(80)	224(27)	−78(86)

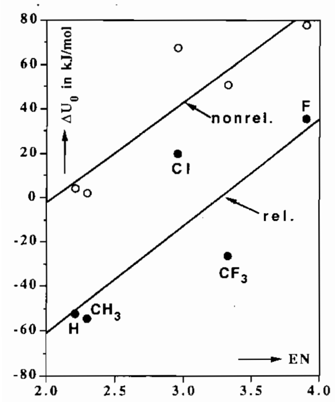

Fig. 5. ΔU_0 values for the disproportionation of $Hg_2X_2 \rightarrow HgX_2 + Hg$ in kJ/mol.

(i) There are large mercury $6p_\sigma$ contributions in the Hg–Hg and Hg–X bonds. Mercury $5d_\sigma$ contributions are relatively small. This contradicts Orgel's suggestion that mercury may prefer ds rather than sp hybridization [60]. π-contributions are rather insignificant (except for $HgCl_2$).

(ii) The Hg spin populations of HgX (Table 7) show that electronegative ligands create a radical centre at the mercury side which will clearly increase the reactivity of this species to form dimeric Hg_2X_2. In contrast, the 'single electron' at $HgCH_3$ is situated at the CH_3 ligand which explains that the preparation of $Hg_2(CH_3)_2$ by the combination of two $HgCH_3$ radicals would be unfavourable. Rather a recombination into C_2H_6 and Hg might occur. The pseudopotential results for the $HgCF_3$ radical show that this species should be more reactive at the metal centre compared to $HgCH_3$. From all the results we may conclude that the reduction of the known compound $Hg(CF_3)_2$ to $Hg_2(CF_3)_2$ should be more feasible than that of $Hg(CH_3)_2$ to $Hg_2(CH_3)_2$.

(iii) Relativistic effects diminish the radical character at the mercury side for all HgX compounds.

The orbital energies for the Hg_2X_2 compounds are collected in Table 8, which may be useful for future work on photoelectron spectra. The bonding behaviour of all compounds can be described qualitatively by the orbital scheme shown in Fig. 6 using Hg(6s) and ligand orbitals. Two linear-combinations of σ_g symmetry are

TABLE 6. MP2 Mulliken orbital populations n_s, n_p and n_d and gross metal charges q for the datomic mercury compounds and their dimers

Molecule		Hg(n_{6s})	Hg(n_{6p_σ})	Hg(n_{6p_π})	Hg(n_{5d_σ})	Hg(n_{5d_π})	Hg(n_{5d_δ})	Hg(q)
HgF	NR	1.08	0.25	0.08	1.99	4.00	3.97	0.56
	R	1.38	0.19	0.08	1.93	3.99	3.97	0.39
HgF_2	NR	0.62	0.24	0.11	1.99	4.07	3.97	0.92
	R	1.02	0.24	0.13	1.89	4.06	3.97	0.65
Hg_2F_2	NR	1.09	0.32	0.09	1.97	4.03	3.97	0.46
	R	1.23	0.31	0.11	1.92	4.01	3.96	0.37
HgCl	NR	1.15	0.30	0.10	1.98	4.01	3.97	0.41
	R	1.50	0.20	0.10	1.93	3.98	3.97	0.23
$HgCl_2$	NR	0.54	0.38	0.19	1.92	4.07	3.97	0.84
	R	0.83	0.40	0.20	1.79	4.02	3.97	0.59
Hg_2Cl_2	NR	0.85	0.58	0.06	1.95	4.03	3.97	0.43
	R	1.12	0.40	0.15	1.90	4.00	3.96	0.38
HgH	NR	1.33	0.40	0.02	1.95	3.97	3.97	0.29
	R	1.65	0.26	0.03	1.90	3.96	3.96	0.15
HgH_2	NR	1.07	0.44	0.02	1.92	3.97	3.97	0.53
	R	1.36	0.42	0.01	1.84	3.95	3.96	0.35
Hg_2H_2	NR	0.98	0.73	0.03	1.93	3.97	3.97	0.31
	R	1.26	0.55	0.04	1.88	3.95	3.96	0.26
$HgCH_3$	NR	1.41	0.33	0.03	1.96	3.97	3.97	0.25
	R	1.94	0.01	0.05	1.98	3.96	3.96	−0.02
$Hg(CH_3)_2$	NR	1.06	0.32	0.05	1.93	3.97	3.97	0.61
	R	1.28	0.30	0.06	1.85	3.96	3.96	0.50
$Hg_2(CH_3)_2$	NR	0.94	0.69	0.05	1.95	3.98	3.97	0.35
	R	1.23	0.52	0.06	1.90	3.95	3.96	0.29
$HgCF_3$	NR	1.48	0.34	0.04	1.97	3.98	3.97	0.15
	R	1.82	0.23	0.06	1.93	3.97	3.96	−0.06
$Hg(CF_3)_2$[b]	NR	0.98	0.46	0.02	2.03	4.06	4.01	0.44
	R	1.28	0.43	0.03	1.93	4.08	4.01	0.23
$Hg_2(CF_3)_2$[b]	NR	0.81	0.74	0.01	2.00	4.03	4.00	0.40
	R	1.17	0.58	0.02	1.97	4.03	4.00	0.22

[a] f contributions are not negligible, i.e. $n_f = 0.09$ for Hg_2F_2 (R). [b] HF only.

TABLE 7. MP2 Mulliken orbital spin populations n_s and n_p and difference of the total α and β spin population (total atomic spin density), $\Delta n(\alpha\beta) = n(\alpha) - n(\beta)$, for various mercury compounds

Molecule HgX		Hg(n_{6s})		Hg(n_{6p})		Hg $\Delta n(\alpha\beta)$	X (=H,F,Cl,C) $\Delta n(\alpha\beta)$
		$n(\alpha)$	$n(\beta)$	$n(\alpha)$	$n(\beta)$		
HgH	NR	0.87	0.46	0.33	0.09	0.67	0.33
	R	0.94	0.72	0.25	0.05	0.46	0.54
HgF	NR	0.93	0.14	0.23	0.09	0.94	0.06
	R	0.98	0.40	0.18	0.09	0.73	0.27
HgCl	NR	0.94	0.22	0.28	0.12	0.89	0.11
	R	1.00	0.50	0.21	0.10	0.64	0.36
$HgCH_3$	NR	0.88	0.54	0.31	0.05	0.62	0.39
	R	0.97	0.97	0.06	0.03	0.03	1.18
$HgCF_3$	NR	0.92	0.56	0.30	0.08	0.60	0.35
	R	0.99	0.84	0.48	0.29	0.38	0.55

responsible for the mercury–mercury bonding, the HOMO showing large Hg(6p) contributions, and the lower lying MO showing some Hg(5d) contributions. Since all three MOs have significant Hg(6s) character, they all are relativistically stabilized. It is interesting, though not surprising that this qualitative MO scheme is almost identical to the MO scheme recently published for $Au_2(PR_3)_2$ [61]. So, Hg_2R_2 is isolobal to $Au_2(PR_3)_2$, as indicated schematically in Fig. 6. Even so, if $Hg_2(CR_3)_2$ is an unknown species (like $Au_2(PR_3)_2$), it may be possible to stabilize this unit on metal centres or cluster compounds as this is the case for $Au_2(PR_3)_2$ [62]. Both fragments, $AuPH_3$ and $HgCH_3$, are rather unstable with a dissociation energy of lower than 10 kJ/mol [61], but become stabilized by dimerization with a dissociation energy of c. 300 kJ/mol for $Au_2(PH_3)_2$ and 125 to 200 kJ/mol for $Hg_2(CH_3)_2$ at the LDA and MP2 levels. Since $AuPR_3$ is often claimed to be isolobal to H [63] (despite some criticism, see ref. 14), the same is true for the $HgCR_3$ fragment. Comparing the two orbital schemes in Fig. 6 we note that the core region containing metal (5d) and ligand (sp) contributions is closer to the three HOMOs in $Au_2(PH_3)_2$ compared to $Hg_2(CH_3)_2$, and that the MOs of $Hg_2(CH_3)_2$ are lying at lower energies compared to $Au_2(PH_3)_2$. We therefore expect some differences in the chemical behaviour of both species. For example, the d-participation in the metal–metal bond is large in $Au_2(PH_3)_2$ but small in $Hg_2(CH_3)_2$.

Figure 7 shows contour plots of the highest lying occupied molecular orbitals of HgH and HgF. In the case of HgH these involve mainly Hg(6s) and H(1s) orbitals whilst for HgF they involve Hg(6s) and F(2p) orbitals. In both cases the singly HOMO has a large Hg(6s) component, this being larger for the HgF molecule. Figure 8 shows contour plots for the high lying occupied molecular orbitals made up from the fragment

TABLE 8. HF orbital energies for Hg and Hg_2X_2 compounds (X=H, F, Cl, CH_3 and CF_3)[a]

Molecule	Sym.	Orbital energy NR/R	Contributions
Hg	6s	−0.261/−0.327	Hg(6s)
	5d	−0.712/−0.606	Hg(5d)
Hg_2H_2	σ_g	−0.289/−0.310	Hg(6s, 6p), H(1s)
	σ_u	−0.387/−0.431	Hg(6s, 6p, 5d), H(1s)
	σ_g	−0.401/−0.461	Hg(6s, 5d), H(1s)
	π_g	−0.714/−0.620	Hg(5d)
	σ_u	−0.716/−0.638	Hg(5d)
	δ_u	−0.732/−0.640	Hg(5d)
	δ_g	−0.736/−0.647	Hg(5d)
	π_u	−0.739/−0.667	Hg(5d)
	σ_g	−0.764/−0.718	Hg(5d)
Hg_2F_2	σ_g	−0.359/−0.430	Hg(6s, 6p), F(2p)
	σ_u	−0.520/−0.532	Hg(6s, 6p, 5d), F(2p)
	π_g	−0.522/−0.540	F(2p), Hg(5d)
	π_u	−0.524/−0.551	F(2p), Hg(5d)
	σ_g	−0.525/−0.545	F(2p), Hg(6s, 5d)
	σ_u	−0.752/−0.686	Hg(5d), F(2p)
	π_g	−0.758/−0.681	Hg(5d), F(2p)
	δ_u	−0.773/−0.689	Hg(5d)
	δ_g	−0.778/−0.698	Hg(5d)
	π_u	−0.787/−0.735	Hg(5d)
	σ_g	−0.807/−0.771	Hg(5d), F(2s2p)
Hg_2Cl_2	σ_g	−0.353/−0.397	Hg(6s, 6p), Cl(3p)
	π_g	−0.425/−0.437	Cl(3p)
	π_u	−0.427/−0.441	Cl(3p)
	σ_u	−0.458/−0.486	Hg(6s, 6p), Cl(3p)
	σ_g	−0.463/−0.507	Hg(6s, 5d), Cl(3s3p)
	σ_u	−0.753/−0.667	Hg(5d), Cl(3s)
	π_g	−0.766/−0.678	Hg(5d)
	δ_u	−0.780/−0.691	Hg(5d)
	δ_g	−0.784/−0.700	Hg(5d)
	π_u	−0.794/−0.732	Hg(5d)
	σ_g	−0.807/−0.757	Hg(5d), Cl(3s)
$Hg_2(CH_3)_2$ (D_{3d})	a_{1g}	−0.273/−0.285	Hg(6s6p), C(2s2p)
	a_{2u}	−0.353/−0.396	Hg(6s6p5d), C(2s2p)
	a_{1g}	−0.374/−0.438	Hg(6s5d), C(2s2p)
	e_g	−0.509/−0.514	C(2p), H(1s), Hg(5d)
	e_u	−0.510/−0.521	C(2p), H(1s)
	a_{2u}	−0.692/−0.603	Hg(5d)
	e_g	−0.706/−0.621	Hg(5d)
	e_u	−0.722/−0.628	Hg(5d)
	e_g	−0.726/−0.636	Hg(5d)
	e_u	−0.730/−0.661	Hg(5d)
	a_{1g}	−0.738/−0.679	Hg(5d)
$Hg_2(CF_3)_2$ (D_{3d})	a_{1g}	−0.322/−0.343	Hg(6s6p), C(2s2p)
	a_{2u}	−0.408/−0.446	Hg(6s6p5d), C(2s2p), F(2p)
	a_{1g}	−0.419/−0.479	Hg(6s5d), C(2s2p)
	a_{2g}	−0.624/−0.638	F(2p)
	a_{1u}	−0.624/−0.638	F(2p)
	e_g	−0.644/−0.648	F(2p)
	e_u	−0.644/−0.657	F(2p)
	e_g	−0.692/−0.667	F(2p)
	e_u	−0.693/−0.677	F(2p)
	a_{2u}	−0.726/−0.651	Hg(6s5d)
	e_g	−0.750/−0.683	Hg(5d)
	a_{1g}	−0.754/−0.711	Hg(5d), F(2p)
	e_u	−0.767/−0.694	Hg(5d)

(*continued*)

TABLE 8. (*continued*)

Molecule	Sym.	Orbital energy NR/R	Contributions
$Hg_2(CF_3)_2$	e_u	−0.770/−0.717	Hg(5d)
(D_{3d})	e_g	−0.770/−0.712	Hg(5d)
	e_g	−0.813/−0.831	C(2p), F(2s2p)
	e_u	−0.814/−0.831	C(2p), F(2p)
	a_{2u}	−0.815/−0.829	Hg(5d), C(2p), F(2p)
	a_{1g}	−0.827/−0.838	Hg(5d), C(2p), F(2p)
	a_{2u}	−0.946/−0.964	Hg(6s), C(2s2p), F(2s2p)
	a_{1g}	−0.947/−0.965	C(2s), F(2s2p)

[a] All values in a.u. Only major contributions and energies above −1.0 a.u. are listed.

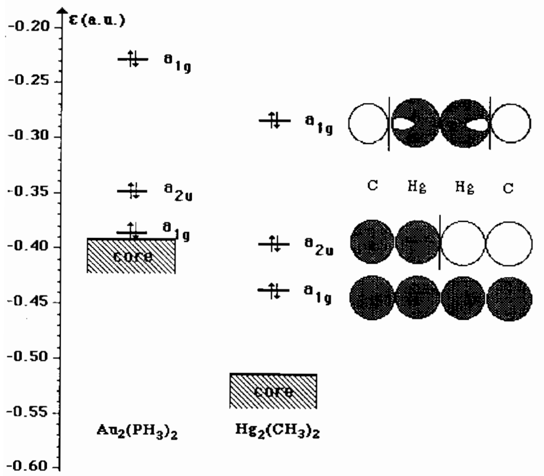

Fig. 6. Comparison of the MO pictures of $Au_2(PH_3)_2$ and $Hg_2(CH_3)_2$.

molecular orbitals of HgH and HgF, respectively. These agree qualitatively with the scheme given in Fig. 7.

4. Conclusions

The stability of the mercury–mercury bond has been investigated by the relativistic pseudopontential and local density approaches. The results can be summarized as follows.

(i) Both the PP and LDA methods give results in quite reasonable agreement with the available experimental data.

(ii) Electronegative substituents support mercury–mercury binding energetically and increase the radical character at the mercury side of HgX, which favours dimerization into Hg_2X_2.

(iii) Relativistic effects strengthen the mercury–mercury bond *but* facilitate the disproportionation of Hg_2X_2 into HgX_2 and Hg.

(iv) $Hg_2(CH_3)_2$ is thermodynamically unstable which explains why organometallic compounds of the form Hg_2R_2 have not yet been prepared. We propose that the preparation of the organometallic compound $Hg_2(CF_3)_2$ might be more feasible, or, that it can more easily be stabilized at other metal centres of cluster compounds.

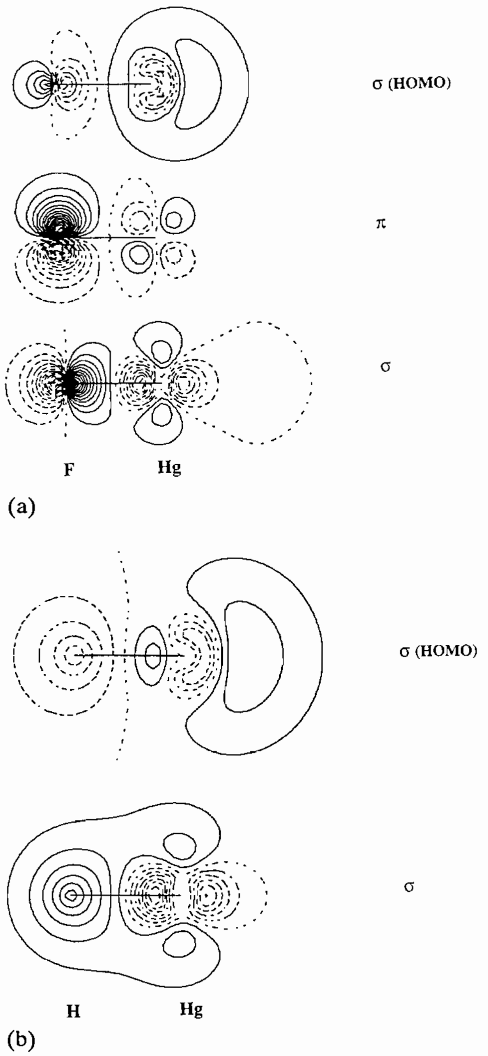

Fig. 7. Contour plots of the high lying occupied molecular orbitals for HgF (a) and HgH (b).

(v) The Mulliken population analysis shows significant Hg(6p) but negligible Hg(5d) participation in the mercury–mercury and mercury–ligand bonds. Of course, the 5d electrons are very important with respect to the electrostatic core potential, Pauli exclusion effects and the core–valence correlation.

This account may not give the final answer to the unique stability of the Hg_2^{2+} ion compared to its lighter Group 12 congeners. More calculations at a higher level, and also including the corresponding Zn and Cd compounds are necessary in order to obtain a quantitative picture of metal–metal bonding in Group 12 compounds. For example, no reduction of Cd^{2+} to Cd_2^{2+} has been achieved yet [1], however, there is

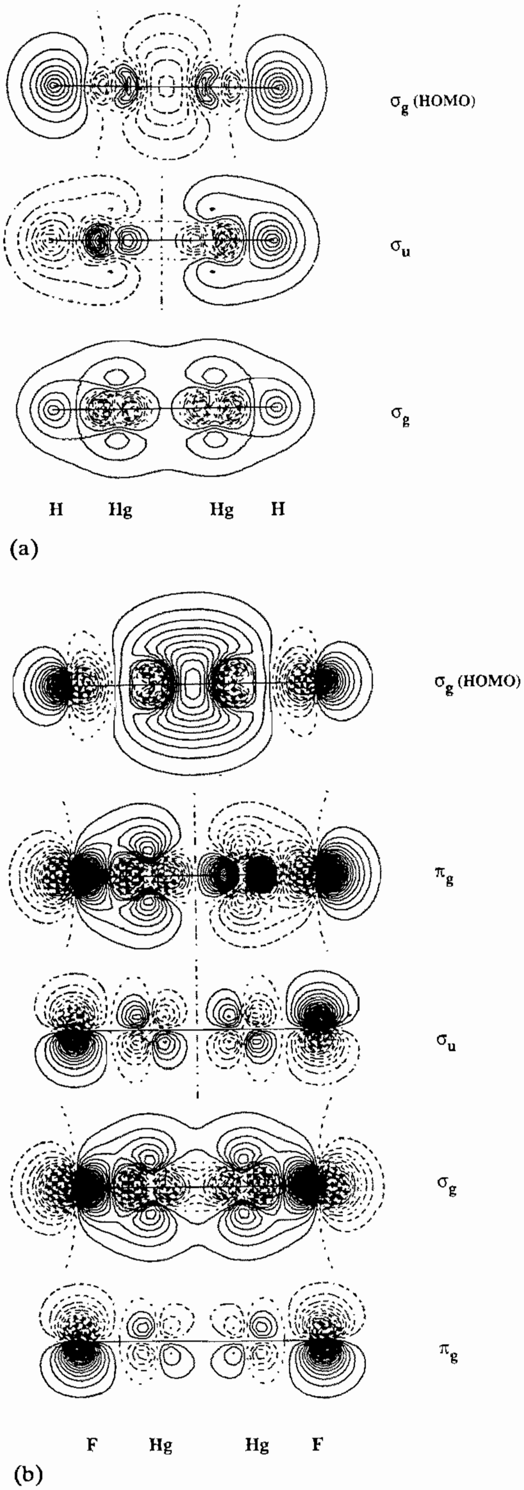

Fig. 8. Contour plots of the high lying occupied molecular orbitals for Hg_2H_2 (a) and Hg_2F_2 (b). The π_u MO of Hg_2F_2 is similar in shape compared to the π_g MO and is therefore not shown.

evidence that Cd_2^{2+} units may exist in Corbett's molten salt $Cd_2(AlCl_4)_2$ [57]. Solvent effects should also be included in order to discuss the stability of Group 12 M_2^{2+} ions [8]. We hope that the present contribution sheds some light on the nature of the mercury–mercury bond.

Acknowledgements

This work was supported by the Alexander von Humboldt Foundation (Bonn), the Auckland University Research Grants Committee, the Lottery Science Board New Zealand, the Deutsche Forschungsgemeinschaft and the Fonds der Chemischen Industrie.

References

1 (a) F.A. Cotton and G. Wilkinson, *Advanced Inorganic Chemistry*, Wiley–Interscience, New York, 5th edn., 1988; (b) K. Brodersen, H.U. Hummel, in G. Wilkinson (ed.), *Comprehensive Coordination Chemistry*, Vol. 5, Pergamon, Oxford, 1987, p. 1047; (c) W.E. Dasent, *Nonexistent Compounds*, Marcel Dekker, London, 1965.
2 E. Dorm, *J. Chem. Soc., Chem. Commun.* (1971) 466.
3 M.S. Liao, *Ph.D. Thesis*, Universität Siegen, Germany, 1993.
4 (a) J. Casanova and H.R. Rogers, *J. Am. Chem. Soc., 96* (1974) 1942; (b) K.P. Butin, A.B. Ershler, V.V. Strelets, A.N. Kashin, I.P. Beletskaya, O.A. Reutov and K. Marcushova, *J. Organomet. Chem., 64* (1974) 171; (c) K.P. Butin, V.V. Strelets, A.N. Kashin, I.P. Beletskaya and O.A. Reutov, *J. Organomet. Chem., 64* (1974) 181; (d) K.P. Butin, V.V. Strelets, I.P. Beletskaya and O.A. Reutov, *J. Organomet. Chem., 64* (1974) 189.
5 Ch. Elschenbroich and A. Salzer, *Organometallics*, VCH, Weinheim, Germany, 1989.
6 D. Strömberg and U. Wahlgren, *Chem. Phys. Lett., 169* (1990) 109.
7 T. Ziegler, J.G. Snijders and J.G. Baerends, *J. Chem. Phys., 74* (1981) 1271.
8 R.P. Neisler and K.S. Pitzer, *J. Phys. Chem., 91* (1987) 1084.
9 Ph. Durand, F. Spiegelmann and A. Bernier, *J. Phys. B, 20* (1987) 1161.
10 P. Pyykkö, *Chem. Rev., 88* (1988) 563.
11 W.H.E. Schwarz, *Theoretical Models of Chemical Bonding*, Vol. 2, Springer, Heidelberg, 1989, p. 593.
12 (a) P. Schwerdtfeger, M. Dolg, W.H.E. Schwarz, G.A. Bowmaker and P.D.W. Boyd, *J. Chem. Phys., 91* (1989) 1762; (b) P. Schwerdtfeger, *Chem. Phys. Lett., 183* (1991) 457.
13 (a) P. Schwerdtfeger, *J. Am. Chem. Soc., 111* (1989) 7261; (b) P. Schwerdtfeger and M. Dolg, *Phys. Rev. A, 43* (1991) 1644; (c) P. Schwerdtfeger, P.D.W. Boyd, S. Brienne and A.K. Burrell, *Inorg. Chem., 31* (1992) 3411.
14 P. Schwerdfeger, P.D.W. Boyd, A.K. Burrell, W.T. Robinson and M.J. Taylor, *Inorg. Chem., 29* (1990) 3593.
15 C.E. Moore, *Atomic Energy Levels*, National Bureau of Standards (US), US GPO, Washington, DC, 1958, Circular No. 467.
16 (a) M. Dolg, U. Wedig, H. Stoll and H. Preuss, *J. Chem. Phys., 86* (1987) 866; (b) D. Andrae, U. Häussermann, M. Dolg, H. Stoll and H. Preuss, *Theor. Chim. Acta, 77* (1990) 123.
17 G.A. Bowmaker and P. Schwerdtfeger, *J. Mol. Struct. (Theochem.), 205* (1990) 295.
18 H. Hosoya, *The Quantum Chemistry Literature Data Base (QCLDB)*, Gakkai Center, Tokyo, Japan, 1992.

19 J.K. Labanowski and J.W. Andzelm, *Density Functional Methods in Chemistry*, Springer, New York, 1991.

20 (a) M. Krauss and W.J. Stevens, *Ann. Rev. Phys. Chem., 35* (1984) 357; (b) S. Huzinaga, *J. Mol. Struct. (Theochem.), 234* (1991) 51.

21 G. Das and A.C. Wahl, *J. Chem. Phys., 64* (1976) 4672.

22 (a) P. Hafner and W.H.E. Schwarz, *J. Phys. B, 11* (1978) 217; (b) *11* (1978) 2975; (c) *Chem. Phys. Lett., 65* (1979) 537.

23 (a) H. Basch, M.D. Newton, J. Jafri, J.W. Moskowitz and S. Topiol, *J. Chem. Phys., 68* (1978) 4005; (b) H. Basch and S. Topiol, *J. Chem. Phys., 71* (1979) 802.

24 (a) W. Schwartmann, *Ph.D. Thesis*, Universität Bochum, Germany, 1979; (b) A. Bernier, Ph. Millié and M. Pelissier, *Chem. Phys., 106* (1986) 195.

25 (a) P.J. Hay, W.R. Wadt, L.R. Kahn and F.W. Bobrowicz, *J. Chem. Phys., 69* (1978) 984; (b) P.J. Hay and W.R. Wadt, *J. Chem. Phys., 82* (1985) 270; (c) M.E. Rosenkrantz, W.J. Stevens, M. Krauss and D.D. Konowalow, *J. Chem. Phys., 72* (1980) 2525; (d) D.B. Neumann and M. Krauss, *J. Chem. Phys., 75* (1981) 315; (e) W.J. Stevens and M. Krauss, *J. Phys. B, 16* (1983) 2921; (f) K.C. Celestino and W.C. Ermler, *J. Chem. Phys., 81* (1984) 1872.

26 D.A. Kleier and W.R. Wadt, *J. Am. Chem. Soc., 102* (1980) 6909.

27 (a) W. Küchle, M. Dolg, H. Stoll and H. Preuss, *Mol. Phys., 74* (1991) 1245; (b) D. Andrae, U. Häussermann, M. Dolg, H. Stoll and H. Preuss, *Theor. Chim. Acta, 77* (1990) 123.

28 (a) M. Dolg, W. Küchle, H. Stoll, H. Preuss and P. Schwerdtfeger, *Mol. Phys., 74* (1991) 1265; (b) U. Häussermann, M. Dolg, H. Stoll, H. Preuss, P. Schwerdtfeger and R.M. Pitzer, *Mol. Phys., 78* (1993) 1211.

29 R.L. DeKock, E.J. Baerends, P.M. Boerrigter and R. Hengelmolen, *J. Am. Chem. Soc., 106* (1984) 3387.

30 (a) J.E. Bice, K.H. Tan, G.M. Bancroft and B.W. Yates, *J. Chem. Phys., 87* (1987) 821; (b) R.L. DeKock, E.J. Baerends, P.M. Boerrigter and R. Hengelmolen, *J. Am. Chem. Soc., 106* (1984) 3387; (c) J.S. Tse, G.M. Bancroft and D.K. Creber, *J. Chem. Phys., 74* (1981) 2097; (d) J.G. Snijders, E.J. Baerends and P. Ros, *Mol. Phys., 38* (1979) 1909; (e) P. Ros, J.G. Snijders and T. Ziegler, *Chem. Phys. Lett., 69* (1980) 297.

31 (a) M.J.S. Dewar and C. Jie, *Organometallics, 8* (1989) 1547; (b) M.J.S. Dewar, G.L. Grady, K.M. Merz and J.J.P. Stewart, *Organometallics, 4* (1985) 1964.

32 P. Schwerdtfeger, *Phys. Scr., 36* (1987) 453.

33 P. Schwerdtfeger, *Ph.D. Thesis*, Universität Stuttgart, Germany, 1986.

34 P. Schwerdtfeger, *J. Am. Chem. Soc., 112* (1990) 2818.

35 (a) G. Peach, in P.G. Burke, W.B. Eissner, D.G. Hummer and I.C. Percival (eds.), *Long Range Interactions in Atoms and Diatomic Molecules, Atoms in Astrophysics*, Plenum, London, 1983; (b) W. Müller, J. Flesch and W. Meyer, *J. Chem. Phys., 80* (1984) 3297.

36 W.H.E. Schwarz, *Acta Phys. Hung., 27* (1969) 391.

37 H. Stoll, P. Fuentealba, M. Dolg, J. Flad, L.v. Szentpály and H. Preuss, *J. Chem. Phys., 79* (1984) 5532.

38 H. Stoll, P. Fuentealba, P. Schwerdtfeger, J. Flad, L.v. Szentpály and H. Preuss, *J. Chem. Phys., 81* (1984) 2732.

39 P. Schwerdtfeger, H. Silberbach and B. Miehlich, *J. Chem. Phys., 90* (1989) 762.

40 K.H. Hellwege, *Landolt-Börnstein, Zahlenwerte und Funktionen aus Naturwissenschaft und Technik*, Springer, Berlin, 1950.

41 P. Schwerdtfeger and G.A. Bowmaker, submitted for publication.

42 (a) R.D. Van Zee, S.C. Blankespoor and T.S. Zwier, *J. Chem. Phys., 88* (1988) 4650; (b) A. Zehnacker, M.C. Duval, C. Jouvet, C. Lardeux-Dedonder, D. Solgadi, B. Soep and O. Benoist d'Azy, *J. Chem. Phys., 86* (1987) 6565.

43 P. Schwerdtfeger, J. Li and P. Pyykkö, *Theor. Chim. Acta*, in press.

44 M.J. Frisch, G.W. Trucks, M. Head-Gordon, P.M.W. Gill, J.B. Wong, J.B. Foresman, B.G. Johnson, H.B. Schlegel, M.A. Robb, E.S. Replogle, R. Gomperts, J.L. Andres, K. Raghavachari, J.S. Binkley, C. Gonzales, R.L. Martin, D.J. Fox, D.J. DeFrees, J. Baker, J.J.P. Stewart and J.A. Pople, *Program GAUSSIAN92*, Revision A, Gaussian Inc., Pittsburgh, PA, 1992.

45 R. Poirier, R. Kari and I.G. Csizmadia, *Handbook of Gaussian Basis Sets*, Physical Sciences Data 24, Elsevier, Amsterdam, 1984.

46 J.A. Pople, M. Head-Gordon and K. Raghavachari, *J. Chem. Phys., 87* (1987) 5968.

47 (a) M.J. Frisch, J.S. Binkley, H.B. Schlegel, K. Raghavachari, C.F. Melius, R. Martin, J.J.P. Stewart, F.W. Bobrowicz, C.M. Rohlfing, L.R. Kahn, D.J. DeFrees, R. Seeger, R.A. Whiteside, D.J. Fox, E.M. Fluder and J.A. Pople, *Program GAUSSIAN86*, Carnegie-Mellon Quantum Chemistry Publishing Unit, Pittsburgh, PA, 1984; extended for local and non-local pseudopotentials by P. Schwerdtfeger using program PSEPOT for the latter: M. Kolar, *Comput. Phys. Commun., 23* (1981) 275; (b) M.J. Frisch, M. Head-Gordon, H.B. Schlegel, K. Raghavachari, J.S. Binkley, C. Gonzales, D.J. DeFrees, D.J. Fox, R.A. Whiteside, R. Seeger, C.F. Melius, J. Baker, R. Martin, L.R. Kahn, J.J.P. Stewart, E.M. Fluder, S. Topiol and J.A. Pople, *Program GAUSSIAN88*, Gaussian Inc., Pittsburgh, PA, 1988; (c) M.J. Frisch, M. Head-Gordon, G.W. Trucks, J.B. Foresman, H.B. Schlegel, K. Raghavachari, M.A. Robb, J.S. Binkley, C. Gonzales, D.J. DeFrees, D.J. Fox, R.A. Whiteside, R. Seeger, C.F. Melius, J. Baker, R.L. Martin, L.R. Kahn, J.J.P. Stewart, S. Topiol and J.A. Pople, *Program GAUSSIAN90*, Gaussian Inc., Pittsburgh, PA, 1990.

48 (a) E.J. Baerends, D.E. Ellis and P. Ros, *Chem. Phys., 2* (1973) 41; (b) J.G. Snijders and E.J. Baerends, *Mol. Phys., 36* (1978) 1789; (c) J.G. Snijders, E.J. Baerends and P. Ros, *Mol. Phys., 38* (1979) 1909; (d) T. Ziegler and A. Rauk, *Theor. Chim. Acta, 46* (1977) 1; (e) T. Ziegler, J.G. Snijders and E.J. Baerends, *J. Chem. Phys., 74* (1981) 1271.

49 S.H. Vosko, L. Wilk and M. Nusair, *Can. J. Phys., 58* (1980) 1200.

50 A.D. Becke, *Phys. Rev. A, 38* (1988) 3098.

51 E.J. Baerends and P. Ros, *Int. J. Quantum Chem. Symp., 12* (1978) 169.

52 (a) C.W. Murray, G.J. Laming, N.C. Handy and R.D. Amos, *Chem. Phys. Lett., 199* (1992) 551; (b) J.A. Pople, P.M.W. Gill and B.G. Johnson, *Chem. Phys. Lett., 199* (1992) 557.

53 P. Vernooijs, J.G. Snijders and E.J. Baerends, Slater type basis functions for the whole periodic system, *Internal Rep.*, Free University, Amsterdam, Netherlands, 1981 and 1992.

54 (a) K.P. Huber, G. Herzberg, *Molecular Spectra and Molecular Structure*, Vol. IV, *Constants of Diatomic Molecules*, Van Nostrand Reinhold, New York, 1979; (b) K.H. Hellwege, *Landoldt-Börnstein, Zahlenwerte and Funktionen aus Naturwissenschaft und Technik*, Vol. 7, Springer, Berlin, 1976; (c) A.D. Mitchell and L.C. Cross, *Tables of Interatomic Distances and Configurations in Molecules and Ions*, The Chemical Society, London, 1958; (d) K. Kashiwabara, S. Konaka, T. Iijima and N.M. Kimura, *Bull. Chem. Soc. Jpn., 46* (1973) 407; (e) K. Kashiwabara, S. Konaka and N.M. Kimura, *Bull. Chem. Soc. Jpn., 46* (1973) 410; (f) H. Skinner, *Modern Aspects of Thermochemistry*, Royal Institute of Chemistry, London, 1958.

55 H. Oberhammer, *J. Mol. Struct.*, *48* (1978) 389.
56 J. Brauer, H. Burger and R. Eujen, *J. Organomet. Chem.*, *135* (1977) 281.
57 (a) J.D. Corbett, W.J. Durkhard, L.F. Druding, *J. Am. Chem. Soc.*, *83* (1961) 76; (b) J.D. Corbett, *Inorg. Chem.*, *1* (1962) 700.
58 N.J. Calos, C.H.L. Kennard and R.L. Davis, *Z. Kristallogr.*, *187* (1989) 305.
59 N. Inamoto and S. Masuda, *Chem. Lett.* (1982) 1003, 1007.
60 L.E. Orgel, *J. Chem. Soc.* (1958) 4186.
61 P. Schwerdtfeger and P.D.W. Boyd, *Inorg. Chem.*, *31* (1992) 327.
62 (a) R.J. Puddephatt, in G. Wilkinson (ed.), *Comprehensive Coordination Chemistry*, Vol. 5, Pergamon, Oxford, 1987, pp. 905–911; (b) M.I. Bruce, *Chem. Aust.*, *57* (1990) 28.
63 (a) J.W. Lauher and J.H. Wald, *J. Am. Chem. Soc.*, *103* (1981) 7648; (b) B.F.G. Johnson, D.A. Kaner, J. Lewis, P.R. Raithby and M.J. Taylor, *Polyhedron*, *1* (1982) 105; (c) D.G. Evans and D.M.P. Mingos, *J. Organomet. Chem.*, *232* (1982) 171.